Journal Pre-proof

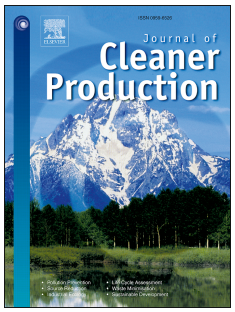

Simultaneous production of biochar and thermal energy using palm oil residual biomass as feedstock in an auto-thermal prototype reactor

Mario A. Heredia Salgado, Jonathan A. Coba S, Luís A.C. Tarelho

PII: S0959-6526(20)31851-5

DOI: https://doi.org/10.1016/j.jclepro.2020.121804

Reference: JCLP 121804

To appear in: *Journal of Cleaner Production*

Received Date: 22 July 2019

Revised Date: 5 March 2020

Accepted Date: 18 April 2020

Please cite this article as: Heredia Salgado MA, Coba S JA, Tarelho LuíAC, Simultaneous production of biochar and thermal energy using palm oil residual biomass as feedstock in an auto-thermal prototype reactor, *Journal of Cleaner Production* (2020), doi: https://doi.org/10.1016/j.jclepro.2020.121804.

Mario A. Heredia Salgado: conceptualization, software, methodology, formal analysis, investigation, writing-Original draft, Visualization, Funding Acquisition, Project Administration, Supervision

Jonathan A. Coba S : formal analysis, investigation, software

Luís A.C Tarelho: conceptualization, methodology, writing-Original draft, writing – review & editing, supervision

Simultaneous production of biochar and thermal energy using palm oil residual biomass as feedstock in an auto-thermal prototype reactor

Mario A. Heredia Salgado[a,b], Jonathan A. Coba S[b], Luís A.C Tarelho[a]

[a] Department of Environment and Planning, Centre for Environmental and Marine Studies (CESAM), University of Aveiro, 3810-193, Portugal

[b] Bioenergía de los Andes (BDA). Gribaldo Miño #4, Quito-Ecuador.

*Corresponding author: heredia.mario@ua.pt (Mario A. Heredia Salgado)

Abstract

In developing countries, the technology used for biomass carbonization requires major retrofits for an efficient conversion of the residual biomass produced in the palm oil mills into biochar. This study analyzes a prototype of a small and modular auger reactor (P-SMART) that uses untreated kernel shells as feedstock to produce biochar and thermal energy. The P-SMART does not require inert gases during operation, neither diesel nor natural gas for the initial heating process. This study shows that the carbonization process can be driven by the energy generated during pyrolysis gas combustion (auto-thermal conditions) from a biomass load capacity of 30 kg/h. During the auto-thermal operation, the thermal energy generated by pyrolysis gas combustion is higher than that required by the carbonization process. The carbon monoxide concentration in the flue gas during the auto-thermal operation was 197 mg/Nm^3 which is lower than the European eco-design requirement of 500 mg/Nm^3 (both measured at 11% vol. O_2, dry gas). The biochars produced during auto-thermal operation have a macro-porous structure with a pore radius that ranges from 0.42 to 12.48 µm. The carbon content and the molar H/C_{org} and O/C_{org} ratio of the analyzed biochars are in accordance with the European guidelines for the sustainable production of biochar of less than 0.7 and 0.4 respectively. Moreover, relevant soil nutrients were observed in the KS ash, namely: silica (30 wt%), potassium (8.2 wt%) and phosphorous (3 wt%).

Keywords

Biochar; Palm oil; Kernel shell; Pyrolysis; Auger reactor; Agro-residues

1. Introduction

Palm oil is an important commodity in the world market because is the most widely used vegetable oil for cooking, food processing, cosmetics, oleo-chemicals and fuels (Oosterveer, 2015). African palm is abundantly planted in tropical regions of Asia, South and Central America where is recognized as an important source of economic growth. Nonetheless, in these regions, the permanent conversion of tropical forests into palm cropland is a major concern (Padfield et al., 2016). Furthermore, the wastes generated in

the mills are recognized as a significant source of water, soil and air pollution (Garcia-Nunez et al., 2015). To prevent the tropical forest deforestation, the sustainability standards promoted by the roundtable on sustainable palm oil (RSPO) has committed the stakeholders throughout the palm oil supply chain including governments, to restrict future expansion of palm oil agriculture to pre-existing cropland or degraded habitats (Roundtable on Sustainable Palm Oil, 2013). However, control over the expansion of the palm oil crop may not be enough to prevent the arising environmental impacts resulting from improper disposal of the wastes generated in the mills.

It is estimated that the residual biomass generated in the mills is around twice the amount of crude palm oil produced (Garcia-Nunez et al., 2016). Generally, palm oil wastes are left scattered at the field sites, which contaminates groundwater through leaching or run-off water and attract air vector-borne diseases (Koh and Wilcove, 2008). Likewise, the decomposition of palm oil residual biomass hoarded at the mills is a significant source of greenhouse gas emissions (Rashidi and Yusup, 2017). Accordingly, the study of alternatives for palm oil wastes valorization is of major relevance. The conversion of palm oil wastes using microwave torrefaction to produce a solid fuel with improved properties and potential to be used in co-firing applications has been suggested (Lam et al., 2019). Nonetheless, a growing interest in palm oil wastes as feedstock for biochar production to be used in several environmental applications has been noticed. This biochar is a carbon rich solid product that can be generated by pyrolysis process, where the raw biomass undergoes thermal decomposition in the absence of O_2, at temperatures typically between 400 °C and 650 °C (Chen et al., 2019). For example, it has been suggested the biochar as with potential to be used for soil amendment (Joseph and Taylor, 2014), as litter or bedding materials (Schmidt et al., 2019), and as animal feed additive (Paz-Ferreiro et al., 2018). Biochar produced by microwave pyrolysis of palm oil shell has shown to be a potential low-cost absorbent for wastewater treatment, as demonstrated by its properties as adsorbent comparable to those of other biochars reported in the literature (Kong et al., 2019). Furthermore, biochar is considered as a tool for carbon sequestration, as a catalyst for chemical reactions, and as an additive in construction materials (Qian et al., 2015).

In tropical regions, biomass carbonization has been traditionally accomplished using brick kilns, retorts and hot tail kilns due to its simplicity and low capital cost (Santos et al., 2017). However, each batch takes more than seven days to be produced, period in which the pyrolytic gases are released directly to the environment (Chidumayo and Gumbo, 2013). It is recognized that the release of pyrolytic gases has a direct impact on air quality and causes the loss of more than 50% of the energy content in the feedstock (Vilela et al., 2014). According to the European guidelines for the sustainable production of biochar, the pyrolytic gases produced during carbonization should be burned to support an energy-autonomous pyrolysis process (European Biochar Foundation, 2018). In this regard, the auger type reactors are an alternative to produce biochar that, keeping simplicity, would overcome the process inefficiencies associated with brick kilns and allow the energetic use of pyrolytic gases (Campuzano et al., 2019). Recent studies show that the direct combustion of the pyrolysis gases generated during the pyrolysis of sewage sludge with a moisture content of 4.6 wt% and LHV of 16.3 MJ/kg in an industrial scale auger reactor can provide the thermal energy required by the carbonization process (Liu et al., 2018). Nonetheless, for the case of wood chips carbonization, a computational fluid dynamic simulation and the following experimental study in a prototype auger reactor have shown that during the combustion process of pyrolysis gas, a pilot flame from e.g. propane combustion is always required to keep steady operating conditions during the pyrolysis process (Woolf et al., 2017). Accordingly, the amount of thermal energy that can be generated in auger type reactors from the combustion of pyrolysis gas would be associated with the feedstock physio-chemical properties, reactor configuration, and operating conditions (Rosas et al., 2014). To the best of the author's knowledge, the carbonization process of residual biomass generated in the palm oil mills in auger type reactors at demonstration scale, e.g., pilot-scale or pre-industrial scale, has not been yet explored. In fact, there is a lack of knowledge about the effectiveness of the carbonization process of palm oil residual biomass (e.g., kernel shell) for biochar production in auger type reactors operating under a auto-thermal and autonomous regime.

Although the use of auger type reactors and the direct combustion of pyrolysis gases could be a major contribution to retrofit the carbonization process in developing countries, it is recognized that further optimization of the pyrolysis gas combustion process is still required for the compliance of international flue gas and particulate matter emissions regulations (Dunnigan et al., 2018). It is observed that some auger type pyrolysis reactors require the integration of flameless oxidation burners in order to control the NO_x emissions that result from direct combustion of pyrolysis gases especially in the cases where the feedstock of the pyrolysis process has high nitrogen content (PYREG, 2018). Moreover, it is recognized that the capital and operating costs of auger type reactors are high because significant electronic and automation controls are required for autonomous operation (Forte et al., 2012). Likewise, the consumption of fossil fuels for the initial starting and heating process of auger type reactors and the use of purge inert gases (e.g., N_2) during operation increase the operating costs (Shackley et al., 2012). The thermo-economic analysis of auger type reactors shows that further costs optimization are required as well as a complete recovery and integration of the waste heat generated during carbonization to adjust the energetic and financial performance so that, the biochar prices can compete in the market with the typical low-cost soil amendments that are used in tropical agriculture (Salgado et al., 2017).

Considering the lack of information about the carbonization process of palm oil residual biomass in auger reactors at pilot-scale and at industrial-scale, this study analyzes the carbonization process of untreated palm oil kernel shells (KS) using a prototype small and modular auger reactor (P-SMART). To the best of the author's knowledge, the demonstration of the carbonization process of residual biomass (kernel shell) generated in the palm oil mills in auger type reactors at pilot-scale and pre-industrial scale for biochar production has not been yet explored. There is a lack of knowledge about the demonstration of the feasibility of this alternative carbonization process of palm oil residual biomass in auger type reactors and on supporting the definition of auto-thermal and autonomous process operating characteristic. Thus, considering the relevance of palm oil industry in the international scenario, the development of knowledge about demonstration at pilot-scale and pre-industrial scale of this integrated thermochemical

(pyrolysis-combustion) alternative for valorization of the wastes (e.g., the kernel shell) from this important agro-industrial sector is significant to promote the sustainable production of palm oil.

The P-SMART integrates three thermochemical conversion processes namely: solid biomass combustion, solid biomass carbonization and pyrolysis gas combustion for the conversion of KS into biochar and thermal energy. In relation to the current status of auger reactors development, this integrated thermochemical conversion system does not require external energy sources as diesel or natural gas for initial heating nor operation. Furthermore, the use of gases to promote an inert atmosphere and drag the pyrolytic gases generated during the carbonization process is avoided. It is worth to highlight that in the P-SMART the KS are feed to the carbonization process with no previous pre-treatment processes like drying, pelletization or particle size reduction. Likewise, the combustion and pyrolysis processes are integrated by modules, which may be of relevance to adapt the pyrolysis process to the rural operations of tropical countries and to decrease the assembly and scale-up operations. In this sense, the P-SMART does not consider complex mechanical parts or advanced casting or cutting technologies, giving priority to the use of materials that are locally available. Indeed, the automation and monitoring controls of the combustion and pyrolysis processes have been developed using open-source hardware and software platforms.

As these characteristics are of relevance in regard to the current status of other auger reactors reported in the literature as well as to advance the integration of thermochemical conversion processes as alternatives for palm oil wastes valorization in tropical countries, this study provides detailed information's about the reactor configuration, ancillaries, and operating stages. Furthermore, this study shows the operating conditions of the KS carbonization process that allow a transition from the initial heating process supported on solid residual biomass combustion, towards a steady operation in auto-thermal conditions, that is, the thermal energy required by the carbonization process is exclusively provided by the combustion of pyrolysis gas. Complementarily, the physio-chemical properties of the biochars produced and the CO concentration in the flue gas observed during the combustion of pyrolysis gas are assessed in

relation to the European guidelines for the sustainable production of biochar (European Biochar Foundation, 2018) and the European eco-design emission standards (The European Commission, 2015a), respectively

2. Materials and methods

2.1. Feedstock characteristics

Although the residual biomass generated in the palm oil mills is diverse, namely empty fruit bunches, mesocarp fibers, kernel shells and palm oil mill effluent, the first demonstration and experimental analysis of the P-SMART considers kernel shells (KS) as feedstock. For the experiments, seven tones of KS were collected from Procepalma, an Ecuadorian palm oil mill located in Quinindé, Santo Domingo de los Tsáchilas province. The collected KS does not have pre-treatment processes as drying, washing or particle size homogenization. The KS particles used in the carbonization experiments are irregular bowl like chips of 5 mm thick and typical size between 6-30 mm. For the experiments, the KS samples were stored in a well-ventilated warehouse sheltered from rain and sun.

2.2. Experimental facility: the prototype of a small and modular auger reactor (P-SMART)

The P-SMART used in the experiments and shown in Figure 1 results from the integration of a previously developed horizontal burner prototype (HBP) and an auger type reactor. The HBP (item 4 in Figure 1) has a power of 30 kW_{th} and produces the thermal energy required during the start-up and initial heating stages of the thermochemical process. The P-SMART integrates a pyrolysis gas burner (PGB) for the energetic conversion (by combustion) of the pyrolysis gas generated during the carbonization process in the pyrolysis reactor (item 5 in Figure1). The thermal energy released from pyrolysis gas combustion fulfills the thermal needs required by the carbonization process, and thus the P-SMART is in auto-thermal operation regime. Details about the operation and combustion efficiency of the HBP can be consulted in the work of Salgado et al. (2019). The HBP and the auger type reactor are integrated through a

combustion chamber (item 6 in Figure 1), where hot gases generated by the HPB, and later by the PGB, heat the pyrolysis reactor. The flue gases that result from the combustion process are discharged to the atmosphere through a chimney (item 12 in Figure 1). The P-SMART combustion chamber has a diameter of 0.65 m, a length of 1.7 m and a 0.15 m thick thermal insulation layer. The pyrolysis reactor has a diameter of 0.33 m and a length of 1.5 m. The effective volume of the combustion chamber, discounting the volume occupied by the pyrolysis reactor is 0.44 m^3.

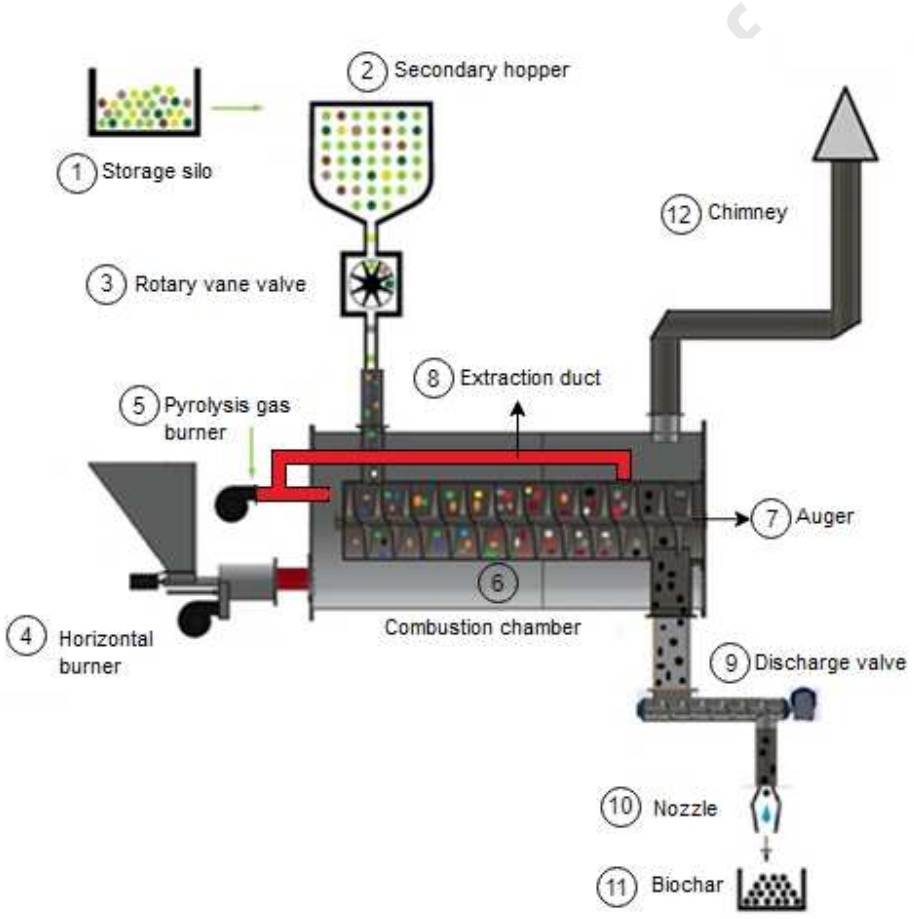

Figure 1. Schematic diagram of the prototype small and modular auger reactor (P-SMART) used in the experiments.

For the carbonization experiments, the KS are fed to the pyrolysis reactor from a hopper (item 2 in Figure 1) through a rotary vane valve (item 3 in Figure 1). The rotary vane valve has special seals to prevent air entrance to the pyrolysis reactor. The KS in the secondary hopper and the rotary vane valve acts as a double air seal. Therefore, the P-SMART does not use additional gases to secure an inert atmosphere in

the pyrolysis process, neither to drag the pyrolytic gases. After the KS passes through the rotary vane valve, the auger rotation (item 7 in Figure 1) moves it along the horizontal axis until the end of the heating zone. The gases generated during the carbonization process are extracted from the pyrolysis reactor and directed towards the PGB by a duct that goes through the hot combustion chamber (see item 8 in Figure 1). The extraction of pyrolysis gas is assisted by a nozzle that accelerates the combustion air fed to the PGB, which is installed within the PGB pre-mixture chamber.

When the KS reaches the end of the pyrolysis reactor, it falls through a discharge port towards a provisional storage hopper. Then, the carbonized KS is discharged from the storage hopper by a time-driven valve (item 9 in Figure 1). During the biochar discharge, the carbonized KS passes through a water spray to prevent dust formation and auto-ignition (item 10 in Figure 1). The operating conditions of the pyrolysis process were defined by three main variables, namely: the mass flow of biomass transported by the auger, the residence time of the biomass in the pyrolysis reactor and the carbonization temperature. The control over activation and rotation speed of the rotary vane valve (see item 3 in Figure 1) allows managing the mass flow of biomass in the pyrolysis reactor. The control over the auger rotation speed allows managing the residence time of biomass in the pyrolysis chamber. Finally, the control over the thermal output power of the HPB or PGB allows controlling the carbonization temperature. The carbonization experiments consider a fixed residence time of 15 minutes and three mass flow levels, namely: 10-30-50 kg/h. Each carbonization experiment lasted around 12 hours which includes the pre-heating stage, the stationary state periods and the cooling period. The P-SMART was operated to perform more than seventy independent experiments that conducted to the processing of more than 4 tons of KS in 1050 hours of operation.

2.3. Electronic controls and monitoring devices associated to the prototype, small and modular auger reactor (P-SMART)

The Figure 2 shows that the P-SMART has two independent controllers, namely: the HBP controller (item 20) and the pyrolysis process controller (item 21). Each controller was developed using an Arduino MEGA 2560 LLC as mainboard which is a commonly used open-source software and hardware prototyping platform (Banzi, 2018). The HBP controller manages the ignition process, operating conditions and thermal output power of the HBP and is described in the work of Salgado et al. (2019). The pyrolysis process controller manages the activation, rotation speed and rotation direction of i) the rotary vane valve, ii) the auger, iii) the discharge valve and iv) the PGB air blower. The residence time of the KS particles in relation to the auger rotation speed was defined by Eq. (1). Where, Δt_r is the KS residence time, Z_p is the total number of auger steps (6 in this case), A_p is the auger pitch (24 cm in this case) and A_v is the auger rotation speed. Thus, the ratio $\frac{A_p}{A_v}$ is the time required by a KS particle to travel the auger pitch distance. Experimental confirmation of the KS residence time in relation to the rotation speed of the auger shaft was done using a chronometer and a dyed control sample.

$$\Delta t_r = Z_p \cdot \frac{A_p}{A_v} \quad (1)$$

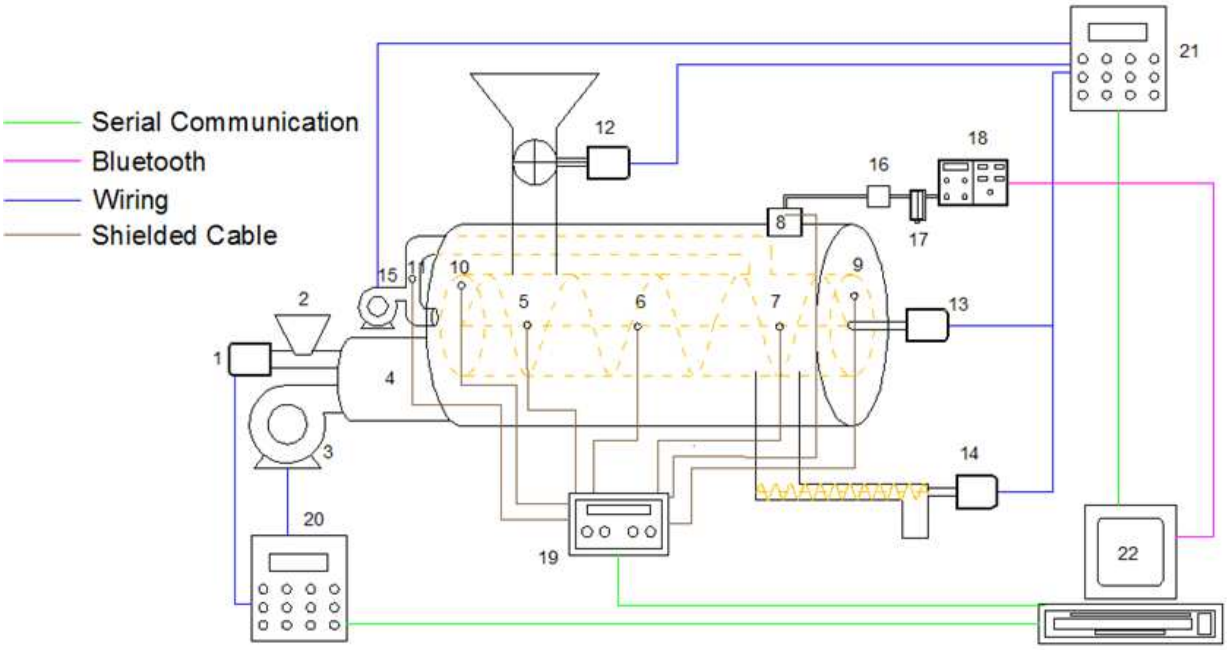

Figure 2. Electronic control and monitoring systems of the P-SMART. Legend: 1. HBP feeder, 2. HBP hopper, 3. HBP blower, 4. HBP frame, 5. Thermocouple (T1), 6. Thermocouple (T2), 7. Thermocouple (T3), 8. Thermocouple (T4), 9. Thermocouple (T5), 10. Thermocouple (T6), 11. Thermocouple (T7), 12. Rotary vane valve motor, 13. Auger motor, 14. Discharge valve motor, 15 PGB blower, 16. Particle filter, 17. Condenser filter. 18. On line gas analyzer 19. Thermocouple data logger, 20. HBP controller, 21. Pyrolysis process controller, 22. Data acquisition

The axial temperature profile in the combustion chamber was monitored using K-type thermocouples of 10 cm long and 5 mm thickness (see items 5, 6, 7 and 8 in Figure 2). The temperatures of the carbonization process were monitored by two K-type thermocouples of (30 cm long, 5 mm thickness) placed through the covers of the pyrolysis reactor (see item 9 and 10 in Figure 2). Furthermore, the pyrolysis gas temperature was monitored by a K-type thermocouple located at the inlet of the PGB (item 11 in Figure 2). The temperatures from the seven thermocouples are acquired every second by the temperature acquisition system (item 19 in Figure 2) and are sent by serial communication to a computer interface (item 22 in Figure 2). Further details of the temperature acquisition system can be found elsewhere (Salgado et al., 2019a). Moreover, the exit flue gas composition during the combustion of pyrolysis gas was monitored in terms of CO, CO_2, HC (expressed as Hexane) and O_2, dry gases, by an AU mobile brain bee infrared online gas analyzer (item 18 in Figure 2). A particle matter filter followed

by a gas condenser submerged in cold water for moisture and condensable material removal were placed before the gas analyzer (item 16 and 17 in Figure 2). The CO emissions during the auto-thermal operation of the P-SMART were assessed according to the European eco-design requirements for solid fuel boilers (The European Commission, 2015b).

2.4. Theoretical considerations for the combustion of pyrolysis gas

The numerical model of Salgado et al. (2018) that uses as input the proximal and elemental composition of the biomass feedstock in order to estimate the changes in the heating value, yield and physio-chemical properties of the pyrolysis gas produced during the carbonization process of KS, was used as reference to define the stoichiometric air-fuel ratio and the excess air rate of the PGB. It is worth to mention that although the KS samples were collected in Quinindé (190 m.a.s.l), the carbonization experiments were performed in Quito (coordinates: S 0°17'30.8" W 78°30'7.9") which corresponding altitude and atmospheric pressure is 2635 m.a.s.l and 99.9 kPa. Accordingly, the calculation of the PGB air/fuel ratio considers an O_2 concentration in the air of 16 %vol, and the corresponding excess air rate to attain the typical O_2 concentration in the exit flue gas during biomass combustion, that is between 8 to 10 % vol. dry gas (Obaidullah et al., 2014). Further details of the numerical models used to estimate the PGB operating conditions can be found in Salgado et al. (2019).

2.5. Analysis of the biochar characteristics and the composition of the KS ash

In order to perform the physical and chemical characterization of the biochar produced in the carbonization experiments, samples of 125 g were taken during the steady-state periods at auto-thermal operation (i.e. the carbonization process is driven exclusively by the thermal energy generated through the combustion of pyrolysis gas). Biochar samples were collected according to the procedure established in the norm UNE-CEN/TS 14778-1:EX. The moisture, ash, and volatile matter content, heating value and C-H-N-S elemental composition of the biochar samples were determined according to the standards: BS EN 14774-3:2009, BS EN 14775:2009, BS EN 15148:2009, ASTM D 1989-96 and BS EN 15104:201.

Morphology of the biochar samples (pore size) and surface chemical composition were characterized by scanning electron microscopy and Energy Dispersive X-Ray Spectroscopy (SEM/EDS, FEI SIRION 200/INCA, OXFORD).

As shown in Figure 1, the HBP use KS as fuel to produce the thermal energy required during the P-SMART initial heating stage. Thus, after the carbonization experiments, samples of 50 g of KS ash were collected from the HBP ash discharge port. The ash samples were cooled at atmospheric air conditions and stored in sealed containers for further analysis. The ash composition was analyzed for the following chemical elements: Sodium, Iron, Calcium, Potassium, and Magnesium. For that purpose, the KS ashes were processed according to the method described in the standard BS EN 15290:2011, namely the acid digestion of the ashes, followed by processing and analysis of the resulting solution for the selected chemical elements using atomic absorption spectrometry (equipment reference ANA-182F) (Silva, 2015).

3. Results and discussion

3.1. Operating stages of the prototype small and modular auger reactor (P-SMART)

The P-SMART integrates three thermochemical conversion processes, namely: residual biomass combustion, residual biomass pyrolysis and combustion of pyrolysis gas. During the initial heating process, the HBP provides the thermal energy required to heat the pyrolysis module using untreated KS as fuel. Thus, the combustion of solid KS particles is the main thermochemical conversion process undergoing at this stage. During the initial heating stage, the temperature fluctuations in the combustion chamber observed every 25 minutes at the location of thermocouples T2 and T3 are caused by the automatic discharge of ashes (see Figure 3A). The ash accumulation in the combustion bed during the HBP operation using KS as fuel requires the periodic activation of the ash removing system to provide proper conditions to sustain the combustion process (Salgado et al., 2019a). In all experiments, the fed of KS to the pyrolysis reactor (carbonization process) starts when the temperature at the inlet of the pyrolysis reactor is around 450 °C (see T6 in Figure 3B). It is observed that the feed of KS at a rate of 30 kg/h to

the pyrolysis reactor causes a decrease in the combustion chamber temperature at time 1h:43min (see T2 and T3 in Figure 3A). Hence, the decrease in the combustion chamber temperature observed at time 1h:43min in Figure 3A, can be attributed to the consumption of energy during the initial steps of biomass carbonization occurring in the pyrolysis reactor once KS is fed, namely drying and devolatilization stages.

At these conditions, the P-SMART starts a transition from the initial heating process towards the co-combustion stage, during which the solid biomass and pyrolysis gas are both burned in the combustion reactor. During this transition, the newly feed KS particles are heated to the operating temperature and distributed along the pyrolysis reactor. This process of KS heating and distribution over the hot pyrolysis bed takes approximately 25 minutes. As the KS particles start to be thermally decomposed during the beginning of the co-combustion stage, the rotation speed of the PGB blower is increased progressively in order to start dragging the pyrolysis gases generated in the pyrolysis chamber towards the combustion chamber. The temperature observed at the inlet of the pyrolysis reactor at the beginning of the co-combustion stage is around 450 °C and could be referred to as the temperature that promotes the decomposition of the KS particle. During the first 30 minutes of the co-combustion stage, several instabilities in the flame front of the PGB are observed as well as a decrease in the temperature at the inlet of the pyrolysis chamber (see T6 in Figure 3B). In this regard, Figure 3B shows that the pyrolysis gas temperature (T7) at the beginning of the co-combustion stage is lower than 300 °C. It is recognized that at low carbonization temperatures the pyrolysis gas would have a low LHV and high water vapor content (Salgado et al., 2018). Thus, the instabilities observed in the PGB flame front at the beginning of the co-combustion stage would be related to the low heating value and high water content associated with the pyrolysis gas generated at this stage of conversion. At the beginning of the co-combustion stage and to compensate for the instabilities observed in the PGB operation, and related to the poor characteristics (e.g., low heating value and high water content) of the pyrolysis gas as fuel at this stage, the thermal energy generated by the HBP supports the evolution of the carbonization process.

At this initial stage of co-combustion operation, the instabilities in the PGB flame front would be also related to the discontinuous flow of pyrolysis gas towards the combustion chamber. A steady flow of pyrolysis gas starts as the temperature in the combustion chamber (see T3 in Figure 3B) is higher than 600 °C. Correspondingly, the temperature at the inlet of the pyrolysis reactor (see T6 in Figure 3B) is close to 450 °C and the pyrolysis gas temperature (see T7 in Figure 3B) approaches to 300 °C. As the temperature in the pyrolysis and combustion processes increase, the LHV of the pyrolysis increase and a more stable flow of pyrolysis gases are fed to the PGB. Accordingly, the temperatures in the combustion and pyrolysis chambers start to rise. In the second half of the co-combustion stage, that is, when the flame front is stabilized at the PGB, the combustion temperature increases promptly to 800 °C (see T3 in Figure 3A). At this condition, the HBP is turned off to give way to the auto-thermal operation regime. It is worth highlighting that the power of the HBP decrease progressively during the co-combustion stage until being completely turned off when the temperature in the combustion chamber (see T3 in Figure 3A) is around 800 °C.

As shown in Figure 3A, at the end of the co-combustion stage the HBP shutdown induces a general temperature decrease in the combustion chamber. However, the combustion chamber temperatures at the location of T2 and T3 stabilize at around 700 °C thereafter. Likewise, the temperature at the inlet and outlet of the pyrolysis reactor stabilizes at around 450 °C and 600 °C respectively (see Figure 3B). At these temperature conditions and considering a load capacity of 30 kg/h and 15 minutes residence time, the pyrolysis process was driven exclusively by the thermal energy generated as result of pyrolysis gas combustion and steady temperature conditions can be observed in the combustion and pyrolysis processes for a period of around 2 hours (see Figure 3).

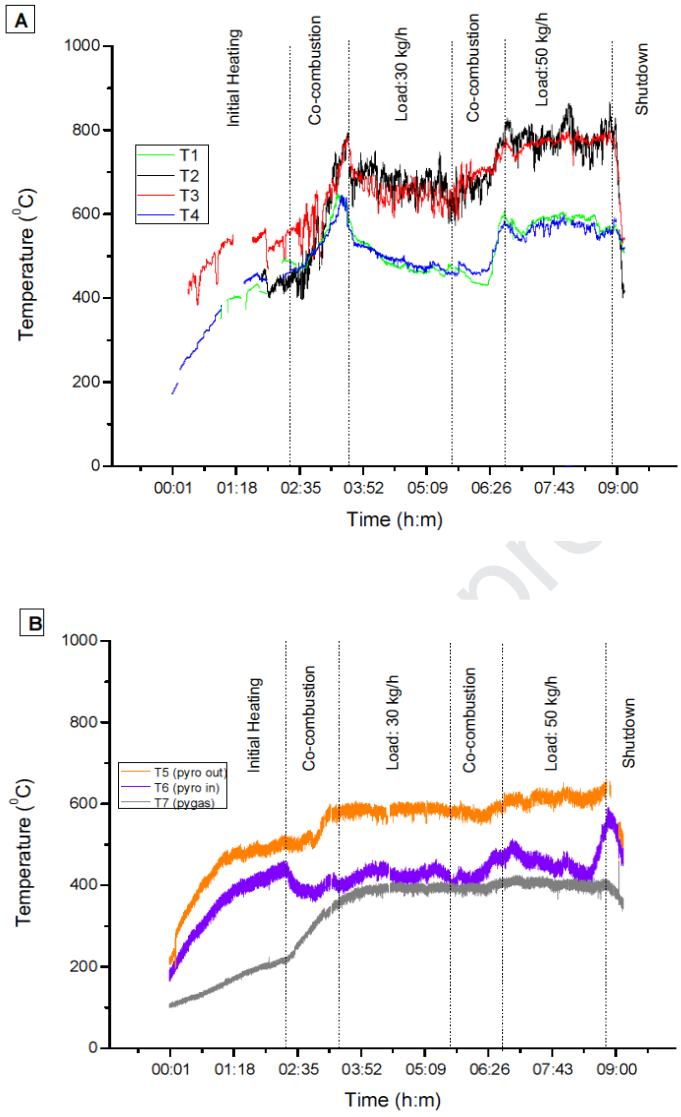

Figure 3. A sequence of the operating stages and the corresponding temperature profiles observed in the combustion (A) and pyrolisis (B) reactors during the carbonization of palm oil kernel shell in the P-SMART. Load capacities: 30 kg/h and 50 kg/h. Kernel Shell residence time: 15 min. Operating stages: initial heating, co-combustion, load 30 kg/h (auto-thermal pyrolysis process), co-combustion and load 50 kg/h (auto-thermal pyrolysis process).

The transition from a load capacity of 30 kg/h to 50 kg/h often results in a sharp decrease of the temperature in the combustion and pyrolysis processes. This temperature decrease may lead to unexpected shutdown events and is caused by the increase in the thermal energy required by the carbonization process that results from the increase in the load capacity. Accordingly, a transition from a

load capacity of 30 kg/h to 50 kg/h requires an energy input to compensate for the increase in the thermal energy consumption of the carbonization process. As shown in Figure 3, after holding for two hours the auto-thermal operation condition at a load capacity of 30 kg/h and 15 minutes residence time, the HBP was turned on to grant the transition from a load capacity of 30 kg/h to 50 kg/h. The Figure 3 shows that the thermal energy input provided by the HBP produces an increase in the combustion chamber temperatures at the location of thermocouples T2 and T3, from 700 °C to almost 800 °C and an increase in the temperatures of the pyrolysis reactor (T5 and T6 in Figure 3B). Then, after de-activation of the HBP, steady-state conditions are observed in the combustion and pyrolysis processes while using exclusively the thermal energy generated by the combustion of pyrolysis gas to drive the carbonization process considering a load capacity of 50 kg/h (residence time of 15 minutes).

During the stages of auto-thermal operation shown in Figure 3, the highest temperatures are observed from the second third of the combustion chamber, at the location of thermocouples T2 and T3. This is related to the progress of combustion along the combustion chamber, reflecting the appropriate air/fuel mixing and subsequent fuel conversion at this location of the reaction chamber. Accordingly, the higher carbonization temperatures are observed in the last third of the pyrolysis reactor that is, at the reactor exit (see T5 in Figure 3B). It should be highlighted that during the auto-thermal operation stages the exit flue gas temperature from the combustion chamber (see T4 in Figure 3A) is higher than 500 °C. The high temperature observed in the flue gas shows that the thermal energy generated as the result of pyrolysis gas combustion is higher than that required by the carbonization process, and this is a common operating condition of continuous pyrolysis units (PYREG, 2018).

It is worth to mention that as part of this study, an individual experiment with a load capacity of 10 kg/h and 15 minutes residence time was considered. Similarly, as the experiment that is shown in Figure 3A, at the end of the initial heating stage with the combustion of KS, a temperature of around 600 °C was reached in the combustion chamber as well as a temperature of 450 °C at the inlet of the pyrolysis reactor. Then, 10 kg/h of KS were fed to the pyrolysis reactor. However, it was observed that the thermal energy

produced by the HBP with a mass flow rate of 8.5 kg/h plus the thermal energy input generated in result of pyrolysis gas combustion was not enough to increase the temperature in the combustion chamber and pyrolysis reactor to values suitable to start the carbonization process, that is, similar to those observed in Figure 3. The inability to increase the temperature in the combustion chamber and pyrolysis reactor to the temperatures observed in Figure 3 is related to the low pyrolysis gas yield from the pyrolysis process corresponding to a KS load capacity of 10 kg/h and a residence time of 15 minutes. As a consequence, no auto-thermal operation could be confirmed using a KS load capacity of 10 kg/h in the pyrolysis reactor.

3.2. Flue gas composition and CO emissions during the P-SMART operation

The CO concentration in the exit flue gas observed during the combustion of KS in the HBP, at an altitude of 2632 m.a.s.l is 260.1 mg/Nm^3 (at 11% vol. O_2, dry gases) which is lower than the European standard for solid fuel-fired boilers and furnaces (500 mg/Nm^3 at 11% vol. O_2, dry gases). Detailed information on the flue gas composition during operation of the HBP, which can be regarded as corresponding to the initial heating stage in the P-SMART under analysis here can be found in Salgado et al. (2019).

The Figure 4 shows that during the first 30 minutes of the co-combustion stage (i.e. solid KS combustion in the HBP and pyrolysis gas combustion in the PGB), the O_2 concentration in the flue gas decreases as the thermal power output of the HBP decreases (see Co-combustion stage in Figure 4). The decrease in the thermal power output of the HBP from 27 kW_{th} to 14 kW_{th} produces a decrease in the volume of flue gases generated from the HBP. Accordingly, the combustion chamber pressure decreases and the pyrolysis gases can be easily dragged from the pyrolysis chamber towards the combustion chamber. The decrease of the O_2 concentration in the flue gas observed in the co-combustion stage of Figure 4 would be then associated to the progressive increase of the pyrolysis gas flow that is fed to the PGB. As observed in Figure 3A, the increase in the pyrolysis gas flow that is fed to the PGB promotes an increase of the temperatures in the combustion and pyrolysis process. The sustained increase of the temperatures in the

combustion and pyrolysis process enhances the thermal decomposition of the KS in the pyrolysis reactor, which supports the increase of the pyrolysis gas flow that is fed to the PGB.

In Figure 4, the peak flow of pyrolysis gas fed to the PGB causes a decrease in the O_2 concentration in the flue gas to almost zero and this is the main reasoning for the high CO and HC concentration observed after 30 minutes of having started the co-combustion stage. Then, once the HBP is turned off, a steady pyrolysis gas flow is achieved in the PGB and a stable flame front is observed. The steady pyrolysis gas flow rate is evidenced by the steady temperatures observed in the combustion chamber after the HBP is turned off (see Figure 3A). At these conditions, the O_2 concentration in the flue gas starts approaching to the theoretical value calculated according to Section 2.4, that is, an average around 10 % vol. dry gases (see PGB flame stabilization in Figure 4). The complete stabilization of the flame front in the PGB after turning off the HBP takes approximately 30 minutes. Then, steady-state conditions are observed while the carbonization process is driven exclusively by the thermal energy generated as the result of pyrolysis gas combustion (see auto-thermal operation stage in Figure 4).

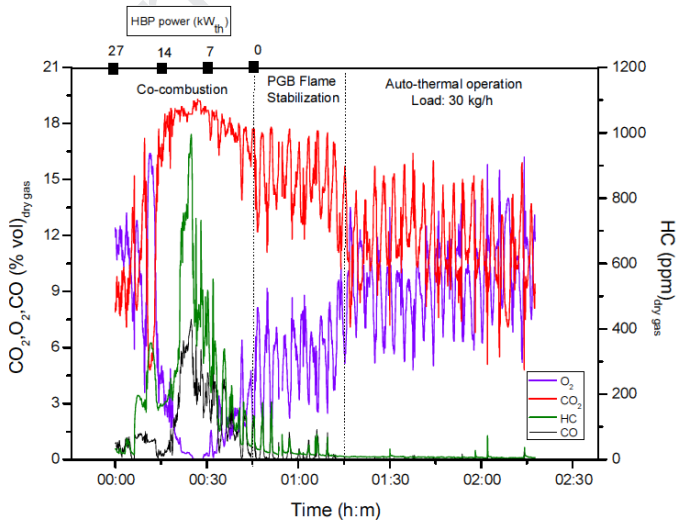

Figure 4. Exit flue gas composition observed during the transition from the co-combustion stage to auto-thermal operation in the carbonization of KS in the P-SMART. Load capacity: 30 kg/h. Residence time: 15 min.

During the auto-thermal operation, the fluctuations in the CO_2 and O_2 concentration in the exit flue gas observed in Figure 4 are associated with the rotary vane valve activation. The pyrolysis process controller is programmed to activate the rotary vane valve 0.5 minute every 4 minutes. This intermittence in biomass feeding to the pyrolysis reactor and the particle movements in the secondary hopper influences the pyrolysis process, namely the release of pyrolysis gas and the corresponding intermittence in gas feeding towards the PGB. During the stand-by period of the rotary vane valve, the pyrolysis gas flow towards the PGB decreases progressively. Once the flow of combustion air provided for the pyrolysis gas combustion process is constant, the intermittent flow of pyrolysis gas to the PGB results in the fluctuations of the CO_2 and O_2 concentration observed in Figure 4. Despite the observed fluctuations in the CO_2 and O_2 concentration in the exit flue gas during the auto-thermal operation, the average O_2 concentration in the exit flue gas was of 9.6 % vol. dry gas and that of CO was of 197 mg/Nm^3 (at 11% vol. O_2, dry gases), which is in accordance with the European CO emission standard of less than 500 mg/Nm^3 (at 11% vol. O_2, dry gases). Therefore, despite these localized and periodic in time CO_2 and O_2 concentration fluctuations, in the whole, and considering longer periods of operation the carbonization process can be regarded as being under steady-state conditions.

3.3. Optimization of the operating conditions during the combustion of pyrolysis gas

For the load capacities of 30 and 50 kg/h the P-SMART was operated under auto-thermal conditions, and the lower CO concentration in the flue gas is observed when the O_2 concentration in the flue gas approaches to 10% vol. dry gas (Figure 5). The CO concentration in the flue gas when the load capacity is of 50 kg/h is higher than that observed at a load capacity of 30 kg/h and higher than the European standard for solid fuel-fired boilers of 500 mg/Nm^3 (at 11% vol. O_2, dry gases). It should be noted that high combustion temperatures close to 733.4 °C were observed during the auto-thermal operation at a load capacity of 50 kg/h (see Figure 3A). Hence, as temperature is within the typical values of combustion processes, the high CO concentration in the flue gas observed may be related to the combustion chamber volume, that is, the combustion gases residence time is too short in relation to the

flow rate of pyrolysis gas that is generated in the carbonization process at a load capacity of 50 kg/h. As stated by Obaidullah et al. (2014), the typical O_2 concentration in the exit flue gas during biomass combustion is in the range between 8 to 10% vol, dry gas. As observed in Figure 5, the result of implementing an O_2 concentration of 8% vol. dry gas is a significant increase in the CO concentration in the flue gas to more than 6000 mg/Nm^3 (at 11% vol. O_2, dry gases). Likewise, an increase in the O_2 concentration in the exit flue gas to more than 10% vol. dry gas also resulted in an increase in the CO concentration.

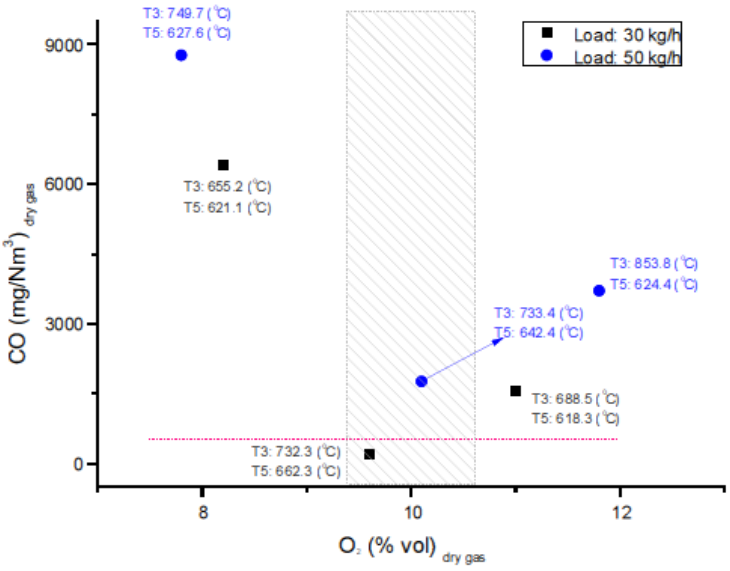

Figure 5. CO concentration calculated according to the European emission standards, as a function of the O_2 concentration in the flue gas. Load capacity of 30 and 50 kg/h. Residence time 15 minutes. Feedstock: palm oil kernel shell. Average pyrolysis gas temperature (T7): 450 °C. The red line shows the European CO concentration limit for solid fuel-fired boilers, 500 mg/Nm^3 (at 11% vol. O_2, dry gases).

3.4. Characteristics of the biochar produced from KS

The SEM micrographs obtained from the biochars produced during auto-thermal operation at 30 and 50 kg/h load capacity (residence time 15 minutes, carbonization temperatures shown in Figure 3B) show a complex pore structure consisting of multiple interconnected networks with different shapes and spatial

arrangements. In general, there are no major differences in the pore sizes between the analyzed biochars (30 kg/h and 50 kg/h). The Figure 6 shows that the morphology of the surface of the biochar particles, including some information on the radius of the observed pores (e.g., size ranges from 0.42 µm to 12.48 µm). Paz-Ferreiro et al. (2018) states that pores with a radius higher than 2.5 µm observed in the biochar are probably part of partially preserved cellular structures. However, the pores with radius in the range from 0.42 to 0.64 µm may be the result of the volatile compounds and tars released during the carbonization process. In the biochar produced at a load capacity of 30 kg/h (reader left side in Figure 6) some big slit-shaped pores/cavities were observed. Brewer et al. (2014) states that slit-shaped pores in biochar may correspond to spaces between graphite-like layers of flat aromatic carbon clusters. The large pore sizes and cavities observed in Figure 6 confirms that the analyzed biochars have a predominant macro-porous structure, which is in accordance with that reported in the literature for biochars produced at high temperatures (Sun et al., 2012).

As shown in Figure 3B the temperature at the inlet of the carbonization process is typical of biochar production, which is 400 °C (Rosas et al., 2014). However, the carbonization temperature at the end of the pyrolysis reactor is around 665 °C, which is significantly higher than the observed in for example electrically heated auger reactors, that is 550 °C (Alburquerque et al., 2016). Thus, the use of high temperatures is relevant to produce a macro-porous biochar, as this type of pores interacts with water to alter soil hydrologic processes, particularly plant-available water and water holding capacity (Liu et al., 2017). Likewise, a well-developed macro-porous structure as that observed in Figure 6 may act as an ecological niche by providing growing space for microorganisms and shelter for mycorrhizal fungi from predators. As stated by Brewer et al. (2014), these micro-organisms are of major relevance to improve soil biogeochemical cycles and subsequently to increase the accessibility of substrates and nutrients to plant roots.

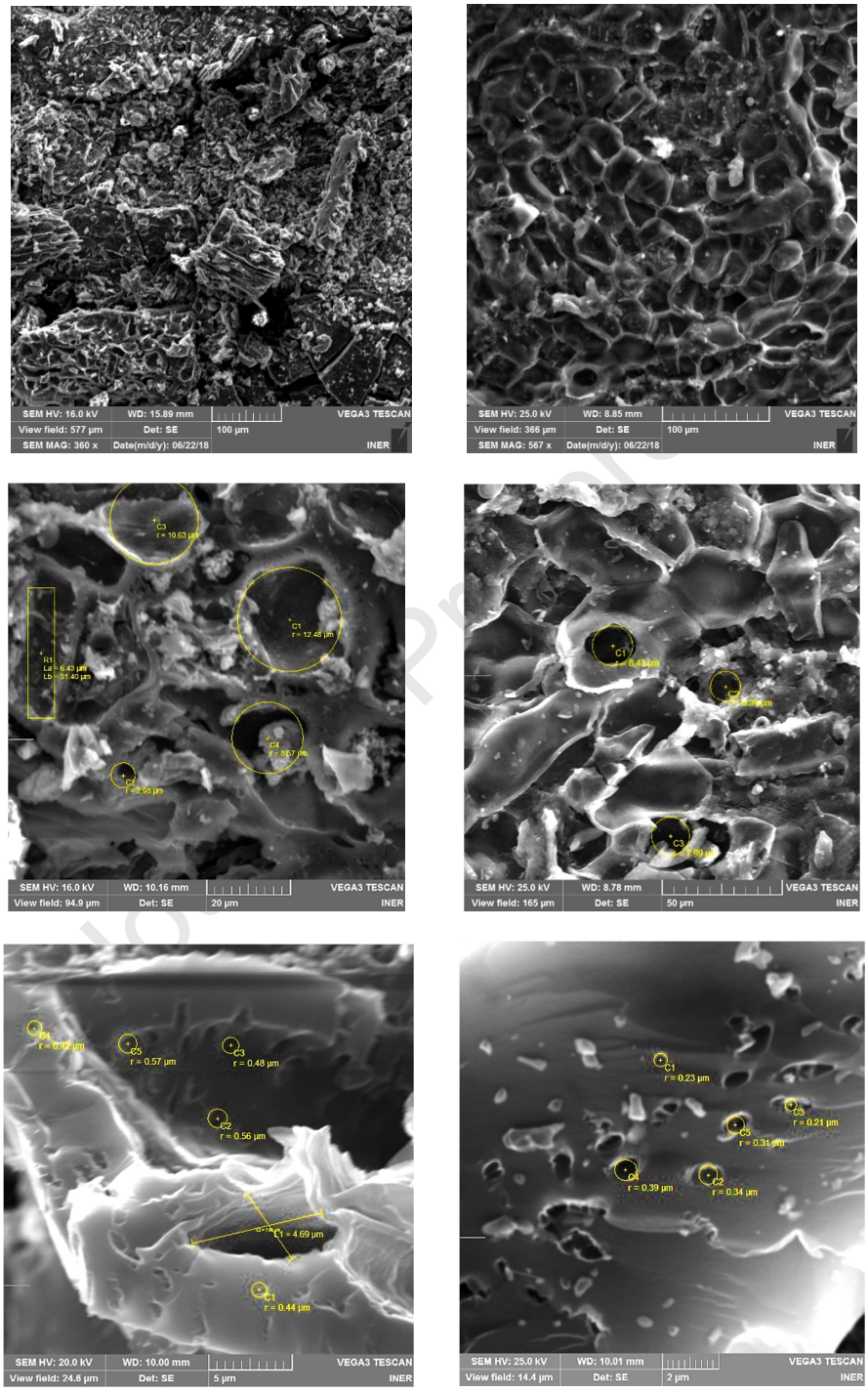

Figure 6. SEM micrographs of KS biochar produced under auto-thermal operating conditions at two different load capacities: 30 kg/h (left side) and 50 kg/h (right side). Residence time: 15 minutes. Carbonization temperatures are shown in Figure 3B.

According to Table 1, the carbon content in the analyzed biochars changes in relation to the operating conditions of the pyrolysis process. Higher carbon content is observed in the biochar produced at a load capacity of 30 kg/h in relation to that observed in the biochar produced at a load capacity of 50 kg/h. As shown in Figure 3B, the increase in the load capacity from 30 to 50 kg/h causes an increase in the carbonization temperature (see thermocouples T5 and T6). However, despite the high carbonization temperatures observed during the auto-thermal operation at a load capacity of 50 kg/h, the increase of the mass transported by the auger presuppose some limitations to transfer the heat produced in the combustion chamber towards the core of the KS particles in the pyrolysis reactor. Accordingly, a lesser carbonization degree can be observed in the biochar produced at a load capacity of 50 kg/h, as can be verified by the higher volatile matter content and lower fixed carbon content in relation to that observed in the biochar produced at a load capacity of 30 kg/h (see Table 1). It is worth to highlight that the carbon content in the analyzed biochars is always higher than 50 wt%, thus in accordance with the guidelines for the sustainable production of biochar (European Biochar Foundation, 2018). The molar H/C_{org} ratio of the analyzed biochars (see Table 1) which is an indicator of the degree of carbonization and therefore of the biochars stability is also within the values established by the guidelines for sustainable production of biochar, namely less than 0.7. Likewise, the O/C_{org} ratio of the analyzed biochars (see Table 1) is lower than 0.4, thus in accordance with the guidelines for the sustainable production of biochar.

Table 1. Proximate and elemental analysis the KS samples collected in the field to perform the carbonization experiments and the biochar produced in auto-thermal operation conditions

Feedstock	**KS**	**Biochar**	
		Load capacity: 30 kg/h	**Load capacity: 50 kg/h**
Proximate Analysis (%wt, wet basis)			
Moisture	12.8	18.4	24
Volatile matter	73.1	7.1	15.9
Ash	2.4	6.1	4.7

Fixed carbon[a]	11.7	68.4	55.4
Ultimate Analysis (%wt, dry basis)			
Ash	2.5	6.5	4.9
C	47.8	78.8	67.5
H	6	2.4	2.7
N	0.6	0.9	0.8
S	nd	nd	nd
O[a]	43.1	11.4	24.1
Lower Heating Value (MJ/kg) (dry basis)	17.7	31.3	30.7
Biochar molar ratios			
H/C_{org}	--	0.4	0.5
O/C_{org}	--	0.1	0.3

[a] Calculated by difference

nd-not determined, bellow the detection limit of the method, 100 ppm (in mass).

The Table 1 shows that as result of the carbonization process the content of the inorganics in the analyzed biochars (ash content in dry basis) almost duplicate and triplicate in relation to that observed in the raw KS. It is observed that the biochar with the higher carbonization degree (i.e. H/C_{org} ratio) has also the higher ash content, that is, the biochar produced at 30 kg/h. It is important to note that if the biochar is used for soil amendment, the ash content of KS may represent the quantity of inorganic elements that would be introduced into the soil. In this regard, the inorganic content in the analyzed biochars may be partially estimated by the elemental analysis of the ashes produced during the KS combustion process in the initial heating stage (see Figure 3A). Of course, the temperatures of the combustion and pyrolysis processes are not the same. At high combustion temperatures, some fraction of the inorganic elements present in the raw KS biomass could volatilize to the gaseous phase and this may lead to misrepresentation of the biochar inorganics content. Considering this clarification, it is observed that the KS ashes have a relatively low concentration of potassium and magnesium when compared to that observed during combustion of biomass from agriculture (Masiá et al., 2007).

As stated by Zeng et al, potassium and magnesium have a highly volatile nature and tend to be released to the gas phase as the combustion temperature increases (Zeng et al., 2016). The high combustion temperatures observed during KS combustion (see Figure 3A) may be the reason for the low potassium and magnesium content in the KS ashes observed in Figure7. The Figure 7 also shows that the ashes that result from the KS combustion have a marginal content of calcium which is typical of ashes that result from the combustion of non-forest waste with high silica content, as for example rice husk (Vassilev et al., 2010). In this study, the SEM/EDS analysis shows that the concentration of silica in the KS ash could be close to 30 wt% (5968 ppm, dry basis). Accordingly, the ash sintering observed during KS combustion in the HBP and previously reported by Salgado et al. (2019) would be related to the silica content in the raw KS and its interaction with other alkaline earth metals as for example potassium. Although the sodium content observed in the KS ashes is low, it is observed that in combination with sodium, the potassium content in the ashes would be promoting a corrosion phenomenon in the combustion equipment, as can be verified through the iron content in the KS ash show in Figure 7. Nevertheless, this subject must be properly characterized in further studies.

It is worth to highlight that silica in free and combined forms is a dominant component of the solid material of many soils. Likewise, silica is absorbed in appreciable quantities by some plants and is returned to the surface of the soil as the plant's decay. Tubana et al., 2016 state that the application of silica fertilizers is very common in many crop production systems worldwide as Si-driven mechanisms enhance the productivity of a wide array of crops even under stress conditions. Accordingly, recycling of silica incorporated within the carbonaceous matrix of KS biochar could be relevant in the context of sustainable management of soils and palm oil crops. However, further research must be made in order to determine the content of metals with environmental relevance as Ni, Cd or Cr, to ensure that the threshold values for application in soils are not exceeded.

It is worth to highlight that the SEM/EDS analysis performed to the analyzed biochars also detected that phosphorous content in the inorganics is around 3 wt%. Unlike the elemental analysis, the SEM/EDS

analysis is not a quantitative analysis technique. Nonetheless, it can be stated that besides sequestering carbon in soils, biochar made from untreated KS may contribute to the recycling of soil nutrients as for example silica, phosphorous, potassium, and magnesium. It is worth to mention that the nutrients in biochar may only be partly available to plants. Camps-Arbestain et al state that the nutrient availability of the phosphorous found in biochar is only 15% during the first year, that of nitrogen a mere 1%, while that of potassium can reach 50% (Camps-Arbestain et al., 2015). Therefore, it should be noted that they may take decades for the inorganics in biochar to enter the biological life cycle.

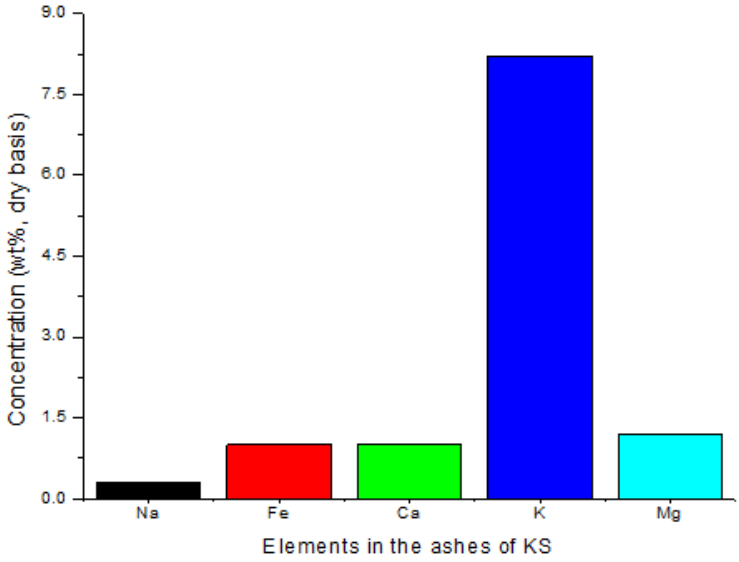

Figure 7. Concentration of sodium, iron, calcium, potassium, and magnesium in the bottom ashes that result from the combustion of KS in the HBP during the initial heating stage of the P-SMART.

It is recognized that the inorganic elements in the biochar may influence its quality. From the elements observed in the KS ash, the biochars made from untreated KS can be defined as sichar because the silica concentration is higher than 5 g per kilogram of biochar (Wang et al., 2019). Accordingly, the sichar made from untreated KS could be used for relevant environmental remediation tasks as for example, to alter the fate of inorganic pollutants in the soils, especially some heavy metals (Xu and Chen, 2014). Hence, the silica observed in the KS ash is of relevance to improve the biochar quality.

4. Conclusions

This study analyzes the carbonization process of untreated kernel shell (KS) in a prototype of a small and modular auger reactor. It is observed that the thermal energy required during the initial starting of the prototype is provided by the combustion of KS in the integrated burner. After the initial starting, the thermal energy required for the carbonization process of KS can be provided through the combustion of pyrolysis gases. No inert gases (e.g., N_2) were required for operation, nor external fuel sources as propane for initial starting and heating of the pyrolysis reactor. Steady auto-thermal operation was observed from a load capacity of 30 kg/h with a residence time of 15 minutes and when the carbonization temperature at the inlet of the pyrolysis reactor is around 450 °C. Furthermore, the thermal energy generated through the combustion of pyrolysis gas is higher than that required by the carbonization process.

The observed carbon monoxide concentration in the flue gas during the combustion of pyrolysis gas was 197 mg/Nm^3 which is lower than the European eco-design standard of 500 mg/Nm^3 (11% vol. O_2, dry gas). The chemical properties of the biochars produced would be in accordance with the European guidelines namely: carbon content higher than 50%, O/C_{org} ratio lower than 0.4 and H/C_{org} ratio lower than 0.7. Likewise, the complementary characteristics of the biochar produced namely, a macro-porous structure that ranges between 0.42 and 12.48 µm as well as the content of inorganics (silica 30 wt%, potassium 8.2 wt%, and phosphorous 3 wt%), would be of relevance in the context of sustainable management of soils and palm oil crops. It is worth to remark that the biochar properties that result from implementing different carbonization temperatures and residence times should be analyzed as well as the use of other wastes generated at the mills as for example mesocarp fibers.

Acknowledgments

This work was supported by the *Instituto de Fomento al Talento Humano*-IFTH and the Republic of Ecuador. The first author acknowledges the IIGE for the support with the flue gas analyzer and the scanning electron microscopy. Thanks are due for the financial support to CESAM

(UID/AMB/50017/2019), to FCT/MCTES through national funds, and the co-funding by the FEDER, within the PT2020 Partnership Agreement and Compete 2020.

References

Alburquerque, J.A., Sánchez, M.E., Mora, M., Barrón, V., 2016. Slow pyrolysis of relevant biomasses in the Mediterranean basin. Part 2. Char characterisation for carbon sequestration and agricultural uses. J. Clean. Prod. 120, 191–197. doi:10.1016/j.jclepro.2014.10.080

Banzi, M., 2018. Arduino [WWW Document]. Arduino Board Softw. URL https://www.arduino.cc/ (accessed 3.15.18).

Camps-Arbestain, Amonette, M., Singh, J.E., Wang, B., Schmidt, T., -P, H., 2015. A biochar classification system and associated test methods, in: Eds (Ed.), Biochar for Environmental Management. Routledge, London, pp. 165–194.

Campuzano, F., Brown, R.C., Martínez, J.D., 2019. Auger reactors for pyrolysis of biomass and wastes. Renew. Sustain. Energy Rev. 102, 372–409. doi:10.1016/j.rser.2018.12.014

Chen, W.H., Wang, C.W., Ong, H.C., Show, P.L., Hsieh, T.H., 2019. Torrefaction, pyrolysis and two-stage thermodegradation of hemicellulose, cellulose and lignin. Fuel 258, 116168. doi:10.1016/j.fuel.2019.116168

Chidumayo, E.N., Gumbo, D.J., 2013. The environmental impacts of charcoal production in tropical ecosystems of the world: A synthesis. Energy Sustain. Dev. 17, 86–94. doi:10.1016/j.esd.2012.07.004

Dunnigan, L., Ashman, P.J., Zhang, X., Wai, C., 2018. Production of biochar from rice husk : Particulate emissions from the combustion of raw pyrolysis volatiles. J. Clean. Prod. 172, 1639–1645. doi:10.1016/j.jclepro.2016.11.107

European Biochar Foundation, 2018. Guidelines for a Sustainable Production of Biochar v4.5E. Eur. Biochar Found. v4.5, 1–22. doi:10.13140/RG.2.1.4658.7043

Forte, B., Coleman., M., Metcalfe, P., Weaver, M., 2012. The case for the PYREG slow pyrolysis process in improving the efficiency and profitability of Anaerobic Digestion plants in the UK [WWW Document]. URL http://www.wrap.org.uk/sites/files/wrap/DIAD I NeueAg feasibility report.pdf

Garcia-Nunez, J.A., Rodriguez, D.T., Fontanilla, C.A., Ramirez, N.E., Silva Lora, E.E., Frear, C.S., Stockle, C., Amonette, J., Garcia-Perez, M., 2016. Evaluation of alternatives for the evolution of palm oil mills into biorefineries. Biomass and Bioenergy 95, 310–329. doi:10.1016/j.biombioe.2016.05.020

Garcia-Nunez, J.A., Rodriguez, D.T., Ramirez, N.E., Silva Lora, E.E., Frear, C.S., Stockle, C., Amonette, J.E., Garcia-Perez, M., 2015. Evolution of Palm Oil Mills into Bio-refinery: Technical and Enviromental Assesments of Six Bio-refinery Options, in: Biorefinery I: Chemicals and Materials From Thermo-Chemical Biomass Conversion and Related Processes.

Joseph, S., Taylor, P., 2014. The production and application of biochar in soils, in: Advances in Biorefineries. Elsevier, South Wales, Australia, pp. 525–555. doi:10.1533/9780857097385.2.525

Koh, L.P., Wilcove, D.S., 2008. Is oil palm agriculture really destroying tropical biodiversity? Conserv. Lett. 1, 60–64. doi:10.1111/j.1755-263X.2008.00011.x

Kong, S.H., Lam, S.S., Yek, P.N.Y., Liew, R.K., Ma, N.L., Osman, M.S., Wong, C.C., 2019. Self-purging microwave pyrolysis: an innovative approach to convert oil palm shell into carbon-rich biochar for methylene blue adsorption. J. Chem. Technol. Biotechnol. 94, 1397–1405. doi:10.1002/jctb.5884

Lam, S.S., Tsang, Y.F., Yek, P.N.Y., Liew, R.K., Osman, M.S., Peng, W., Lee, W.H., Park, Y.K., 2019. Co-processing of oil palm waste and waste oil via microwave co-torrefaction: A waste reduction

approach for producing solid fuel product with improved properties. Process Saf. Environ. Prot. 128, 30–35. doi:10.1016/j.psep.2019.05.034

Liu, X., Chang, F., Wang, C., Jin, Z., Wu, J., Zuo, J., Wang, K., 2018. Pyrolysis and subsequent direct combustion of pyrolytic gases for sewage sludge treatment in China. Appl. Therm. Eng. 128, 464–470. doi:10.1016/j.applthermaleng.2017.08.091

Liu, Z., Dugan, B., Masiello, C.A., Gonnermann, H.M., 2017. Biochar particle size, shape, and porosity act together to influence soil water properties. PLoS One 12, 1–19. doi:10.1371/journal.pone.0179079

Masiá, A.A.T., Buhre, B.J.P., Gupta, R.P., Wall, T.F., Palm, B., 2007. Characterising ash of biomass and waste. Fuel Process. Technol. 88, 1071–1081. doi:10.1016/j.fuproc.2007.06.011

Obaidullah, M., Dyakov, I. V., Thomassin, J.D., Duquesne, T., Bram, S., Contino, F., De Ruyck, J., 2014. CO emission measurements and performance analysis of 10 kW and 20 kW wood stoves. Energy Procedia 61, 2301–2306. doi:10.1016/j.egypro.2014.12.443

Oosterveer, P., 2015. Promoting sustainable palm oil: viewed from a global networks and flows perspective. J. Clean. Prod. 107, 146–153. doi:10.1016/j.jclepro.2014.01.019

Padfield, R., Drew, S., Syayuti, K., Page, S., Evers, S., Campos-Arceiz, A., Kangayatkarasu, N., Sayok, A., Hansen, S., Schouten, G., Maulidia, M., Papargyropoulou, E., Tham, M.H., 2016. Landscapes in transition: an analysis of sustainable policy initiatives and emerging corporate commitments in the palm oil industry. Landsc. Res. 41, 744–756. doi:10.1080/01426397.2016.1173660

Paz-Ferreiro, J., Nieto, A., Méndez, A., Askeland, M.P.J., Gascó, G., 2018. Biochar from biosolids pyrolysis: A review. Int. J. Environ. Res. Public Health 15. doi:10.3390/ijerph15050956

PYREG, 2018. The PYREG® process [WWW Document]. Mater. Therm. Recycl. Org. residues. URL

https://www.pyreg.de/ (accessed 12.10.18).

Qian, K., Kumar., A., Zhang, H., Bellmer, D., Huhnke, R., 2015. Recent advances in utilization of biochar. Renew. Sustain. Energy Rev. 42, 1055–1064. doi:10.1016/j.rser.2014.10.074

Rashidi, N.A., Yusup, S., 2017. A review on recent technological advancement in the activated carbon production from oil palm wastes. Chem. Eng. J. 314, 277–290. doi:10.1016/j.cej.2016.11.059

Rosas, G., Cara, J., Martínez, O., 2014. Slow pyrolysis of relevant biomasses in the Mediterranean basin . Part 1 . Effect of temperature on process performance on a pilot scale. J. Clean. Prod. 120, 181–190. doi:10.1016/j.jclepro.2014.10.082

Roundtable on Sustainable Palm Oil, 2013. Principles and Criteria for the Production of Sustainable Palm Oil [WWW Document]. Draft Colomb. Natl. Interpret. 2013 Stand.

Salgado, M.A.H., Tarelho, L.A.., Matos, M.A.A., Rivadeneira, D., Narváez C, R.A., 2019a. Palm oil kernel shell as solid fuel for the commercial and industrial sector in Ecuador: tax incentive impact and performance of a prototype burner. J. Clean. Prod. 213, 104–113. doi:10.1016/j.jclepro.2018.12.133

Salgado, M.A.H., Tarelho, L.A.C., Matos, A., 2018. Analysis of Combined Biochar and Torrefied Biomass Fuel Production as Alternative for Residual Biomass Valorization Generated in Small-Scale Palm Oil Mills. Waste and Biomass Valorization 9, 1–14. doi:10.1007/s12649-018-0467-7

Salgado, M.A.H., Tarelho, L.A.C., Matos, A., Robaina, M., Narváez, R., Peralta, M.E., 2017. Thermoeconomic analysis of integrated production of biochar and process heat from quinoa and lupin residual biomass. Energy Policy 114, 332–341. doi:10.1016/j.jhep.2009.07.006

Salgado, M.A.H., Tarelho, L.A.C., Rivadeneira-Rivera, D.A., Ramirez, V., Sinche, D., 2019b. Energetic valorization of the residual biomass produced during Jatropha curcas oil extraction. Renew. Energy

146, 1640–1648. doi:https://doi.org/10.1016/j.renene.2019.07.154

Santos, S.D.F. de O.M., Pierkarski, C.M., Ugaya, M.L., Donato, D.B., Júnior, A.B., Francisco, A.C. De, Carvalho, A.M.M.L., 2017. Life Cycle Analysis of Charcoal Production in Masonry Kilns with and without Carbonization Process Generated Gas Combustion. Sustainability 8, 1558-. doi:https://doi.org/10.3390/su9091558

Schmidt, H.P., Anca-Couce, A., Hagemann, N., Werner, C., Gerten, D., Lucht, W., Kammann, C., 2019. Pyrogenic carbon capture and storage. GCB Bioenergy 11, 573–591. doi:10.1111/gcbb.12553

Shackley, S., Hammond, J., Gaunt, J., Ibarrola, R., 2012. The feasibility and costs of biochar deployment in the UK. Carbon Manag. 3, 335–356. doi:10.4155/cmt.11.22

Silva, D.F.R., 2015. Valorização das cinzas de combustão de biomassa na calagem e reciclagem de nutrientes no solo. Universidade de Aveiro.

Sun, H., Hockaday, W.C., Masiello, C.A., Zygourakis, K., 2012. Multiple Controls on the Chemical and Physical Structure of Biochars. Ind. Eng. Chem. Res. 51, 3587–3597. doi:10.1021/ie201309r

The European Commission, 2015a. COMMISSION REGULATION (EU) 2015/1189: implementing Directive 2009/125/EC of the European Parliament and of the Council with regard to ecodesign requirements for solid fuel burners. Off. J. Eur. Union L193/100, 8–15.

The European Commission, 2015b. COMMISSION REGULATION (EU) 2015/1188: implementing Directive 2009/125/EC of the European Parliament and of the Council with regard to ecodesign requirements for local space heaters. Off. J. Eur. Union L193/76, 1–19.

Vassilev, S. V., Baxter, D., Andersen, L.K., Vassileva, C.G., 2010. An overview of the chemical composition of biomass. Fuel 89, 913–933. doi:10.1016/j.fuel.2009.10.022

Vilela, A. de O., Lora, E.S., Quintero, Q.R., Vicintin, R.A., Pacceli da Silva e Souza, T., 2014. A new

technology for the combined production of charcoal and electricity through cogeneration. Biomass and Bioenergy 69, 222–240. doi:10.1016/j.biombioe.2014.06.019

Wang, Y., Xiao, X., Xu, Y., Chen, B., 2019. Environmental Effects of Silicon within Biochar (Sichar) and Carbon-Silicon Coupling Mechanisms : A Critical Review. Environ. Sci. Technol. doi:10.1021/acs.est.9b03607

Woolf, D., Lehmann, J., Joseph, S., Campbell, C., Christo, F.C., Angenent, L.T., 2017. An open-source biomass pyrolysis reactor. Biofuels, Bioprod. Biorefining 11, 945–954. doi:https://doi.org/10.1002/bbb.1814

Xu, Y., Chen, B., 2014. Organic carbon and inorganic silicon speciation in rice-bran-derived biochars affect its capacity to adsorb cadmium in solution. J. Soils Sediments 15, 60–70. doi:10.1007/s11368-014-0969-2

Zeng, T., Weller, N., Pollex, A., Lenz, V., 2016. Blended biomass pellets as fuel for small scale combustion appliances: Influence on gaseous emissions and total particulate matter emissions and applicability of fuel indices. Fuel 184, 689–700. doi:10.1016/j.fuel.2016.07.047

Nomenclature

Abbreviations

HBP	Horizontal burner prototype
KS	Kernel shell
LHV	Lower heating value
m.a.s.l	Meters above the sea level
PGB	Pyrolysis gas burner
P-SMART	Prototype small and modular auger reactor
RSPO	Round table on sustainable palm oil
USD	United states dollars

Subscripts

db	Dry basis
wb	Wet basis

Symbols		Units
wt%	Weight percentage	%
Δt_r	Residence time	min
Z_P	Auger steps	-
A_P	Auger pitch	cm
A_v	Auger rotation speed	cm/min

1

2

3

Highlights

- No external sources as diesel or natural gas were used for heating or operation
- No inert gases were used to promote an inert atmosphere or drag the pyrolytic gas
- The carbonization process is autothermal for biomass loads over 30 kg/h
- The characteristics of the biochars produced are within the European guidelines
- The kernel shell ash is rich in silica, potassium, and phosphorous

Declaration of interests

☒ The authors declare that they have no known competing financial interests or personal relationships that could have appeared to influence the work reported in this paper.

☐The authors declare the following financial interests/personal relationships which may be considered as potential competing interests: